Project in Space Physics at Uppsala University and the Swedish Institute of Space Physics

The electron density in Saturn's magnetosphere around equinox

Klaus Gwosch*

June 14, 2010

Supervisor: Michiko Morooka

*E-mail: Gwosch@stud.uni-heidelberg.de

Abstract

This report presents an analysis of the electron density in Saturn's magnetosphere around equinox (August 11, 2009). The electron density was derived from the spacecraft potential which was determined by the Langmuir probe on-board the Cassini spacecraft. The floating potential can be used as a proxy for the ambient electron density in tenuous plasmas, cf. Morooka et al. [MMW+09].

The electron density showed a disc-like structure which was aligned with the equatorial plane of Saturn. The density decreases with increasing distance from Saturn as well as with increasing distance from the equatorial plane. In addition the density showed a longitudinal asymmetry with a periodicity close to the rotation period of Saturn.

The density distribution was compared with the study of Morooka et al. where the plasma disc on the nightside was shifted to the northern hemisphere for dipole L-values beyond $15\,R_S$. In this study the plasma disc seems to be more aligned with the equatorial plane, even at those distances. This is probably due to the fact that the solar wind is aligned with the equatorial plane at equinox, thus it does not push the plasma out of the equatorial plane.

In this study the Cassini orbits 099 to 126 were analysed, covering the time interval from December 31, 2008 to February 22, 2010.

Contents

1 Introduction

At this date the Cassini-Huygens spacecraft (s/c) is orbiting Saturn and studying the Saturnian system. On-board is a Langmuir probe (LP) which is operated by the Swedish Institute of Space Physics (IRF) and measures properties like density, temperature, flow speed and mean ion mass of the ambient plasma. One interesting parameter is the electron density which can be measured by the LP in different ways, one of these uses the LP floating potential U_{float}. The floating potential depends directly on the spacecraft potential $U_{s/c}$ which can be used as a proxy for the electron density in a tenuous plasma. In this study this is used to determine the electron distribution in Saturn's magnetosphere during the time around equinox (August 11, 2009).

The purpose of this study is to obtain a general distribution of Saturn's magnetospheric plasma. This is compared with previous studies, especially with the study of M. W. Morooka et al. [MMW+09], to see if there is a seasonal dependence.

The electron distribution around Saturn shows a disc-like structure with the highest density in the equatorial region. The density decreases with increasing distance from the equatorial plane as well as with increasing distance from Saturn. The distribution shows in addition a longitudinal asymmetry co-rotating with Saturn.

Included in this report is a short description of Saturn's environment, the Cassini-Huygens spacecraft and the Langmuir probe (section 2). The analysis method is presented in section 3 and the results can be found in section 4. Section 5 includes a summary and some suggestions on improvements and for further investigations.

2 Saturn's magnetosphere and the instrument

2.1 Saturn's magnetosphere

Saturn is is one of the gas giants in our solar system and consists mainly of hydrogen and helium. It is located about 9.5 AU from the Sun and is built up around a small core of rock and ice surrounded by a thick layer of metallic hydrogen. Outside the metallic layer of hydrogen is a gaseous layer consisting mainly of hydrogen, some helium and trace elements. The metallic hydrogen is the source of a very strong dipole-like magnetic field with the dipole axis closely aligned with the axis of planetary rotation (tilt smaller than 1 °) [Sat09]. The rotation period of Saturn is ∼10.7 h which is about 2.5 times faster than that of Earth. The equatorial radius of Saturn is about $6 \cdot 10^4$ km which is about ten times larger than the radius of Earth. The large radius and the fast rotation are the reason for strong centrifugal forces at Saturn's equator, which has a large effect on the plasma in Saturn's magnetosphere. The plasma originates mainly from internal plasma sources like the rings and icy moons, especially Enceladus [PGK+05]. Due to the centrifugal force the plasma tends to concentrate around the magnetic equator. The density decreases with increasing distance from Saturn, as well

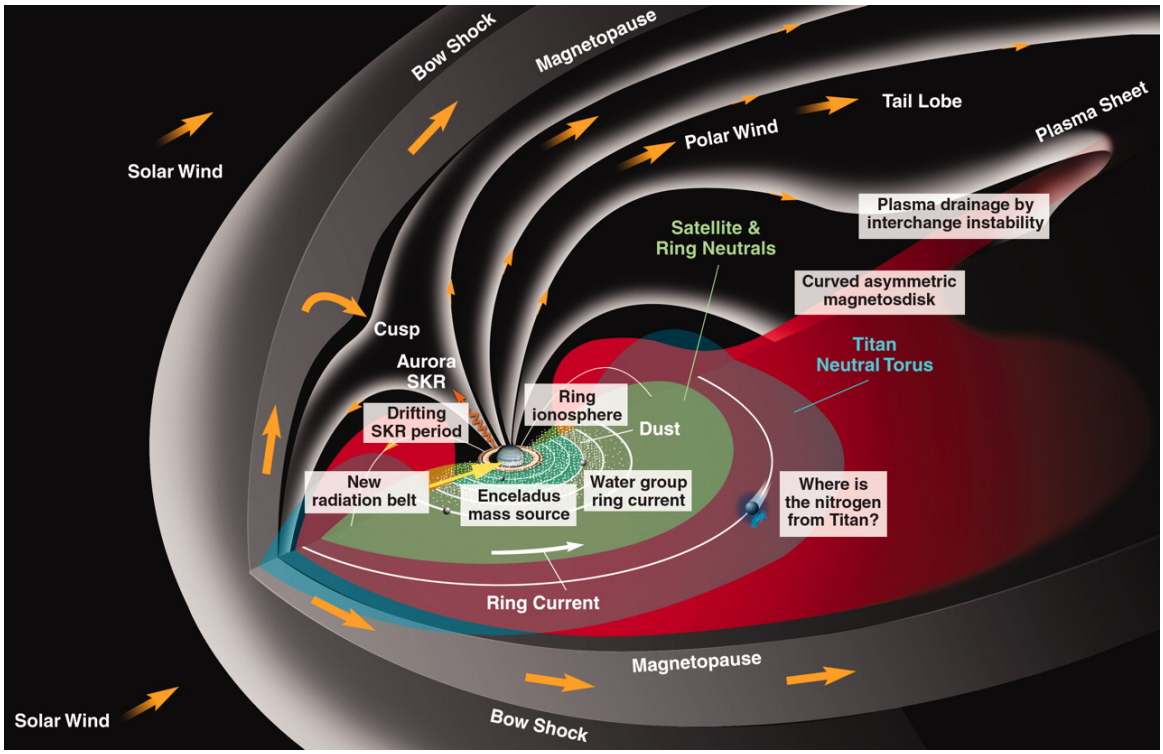

Figure 1: Saturn's magnetosphere with some of the new discoveries from the Cassini Prime Mission. The picture is taken from the paper of Tamas I. Gombosi et al. [GI10].

as from the equatorial plane.

The current model for Saturn's magnetosphere is illustrated in figure 1 including some of the new discoveries from the Cassini Prime Mission.

Previous studies, e.g. Morooka et al. [MMW+09] and Arridge et al. [AKR+08], found that the plasma disc is shifted to the northern hemisphere in the magnetospheric tail. This is probably due to interactions of the solar wind with the magnetosphere that result in a force on the plasma disc which pushes it to higher latitudes. The shape of the plasma sheet in such a distorted magnetosphere is shown in figure 2. In equinox the solar wind is aligned with the magnetic equator and one expects the plasma sheet to be aligned with the equator. This results in a slower decrease of the density in the equatorial plane with increasing distance from Saturn, see also section 4.2.

[Hol10]

2.2 The Cassini spacecraft

The Cassini-Huygens is a mission of NASA, ESA and ASI mainly to study the planet Saturn and its moons, especially Titan. The mission consists of two spacecraft (figure 3), the Cassini orbiter (NASA) and the Huygens probe (ESA). It was launched on October 15, 1997 and entered after several planetary swing-bys into orbit around

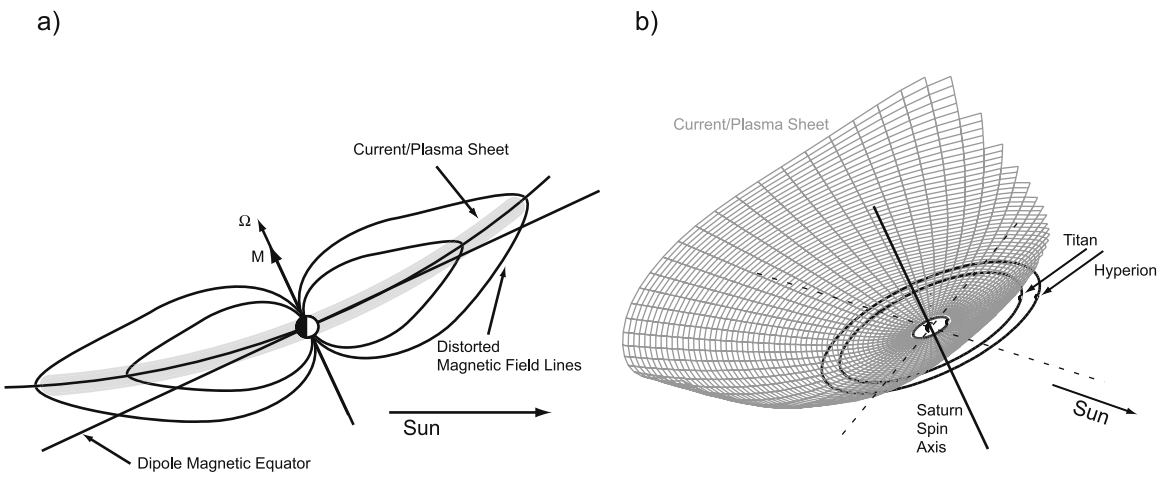

Figure 2: Schematics illustrating the distortion of Saturn's magnetosphere at times far away from equinox. The picture is taken from Arridge et al. [AKR+08].

Saturn on July 1, 2004. The Huygens probe successfully landed on the moon Titan on January 14, 2005. It made several measurements of Titan's atmosphere as well as of its surface.

The Cassini orbiter is still in orbit around Saturn, where it performs measurements of Saturn's environment and the icy moons, mainly Enceladus and Titan. The mission is planed to continue to 2017. The orbiter is 6.7 m high and 4 m wide and has a weight of 2125 kg (unfueled) and 5712 kg with fuel, Huygens probe, adapter, etc.. It is equipped with 12 scientific instruments and is powered by three Radioisotope Thermoelectric Generators (RTG). Four instruments (CIRS, ISS, UVIS and VIMS) are for optical remote sensing, six instruments to study fields, particles and waves (CAPS, CDA, INMS, MAG, MIMI and RPWS) and two instruments (Radar and RSS) are used for microwave remote sensing [JPL].

In this study the measurements of the Langmuir probe, which is part of the Radio and Plasma Wave Science (RPWS) instrument, are used. Its function is described in section 2.3. The Langmuir probe can be seen in figure 3.

2.3 Langmuir probe and floating potential

The Langmuir probe (LP) is a part of the Radio and Plasma Wave Science (RPWS) instrument on-board Cassini. It was developed by the Swedish Institute of Space Physics in Uppsala and measures parameters like density and temperature of the ambient plasma electrons and ions.

The Langmuir probe consists of a metallic sphere about 50 mm in diameter with a titan nitride surface coating and is mounted on a 1.5 m boom. The basic principle of a Langmuir probe is to set the probe to a negative or positive potential and measure the current. The measurements are performed as voltage sweeps (see figure 4), or as

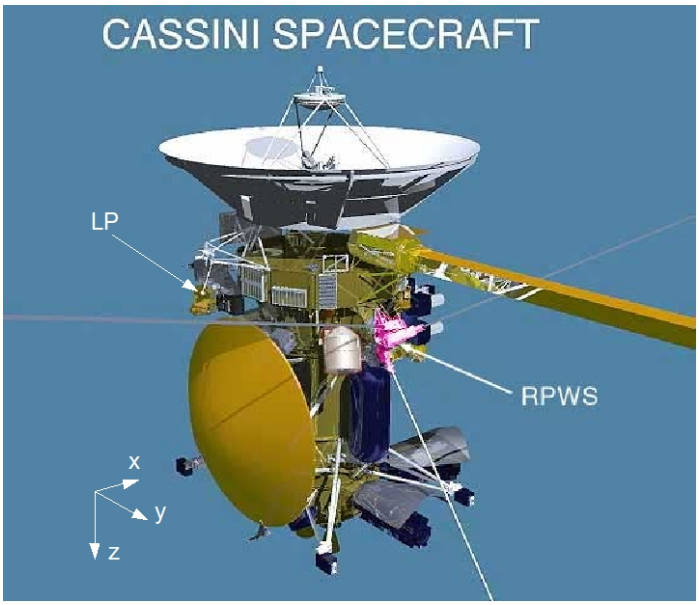

Figure 3: The Cassini-Huygens spacecraft. The Langmuir probe (LP) is mounted almost in negative $X_{s/c}$-direction. The gold-coloured part below the LP is the Huygens probe. Source: http://saturn.jpl.nasa.gov/spacecraft/cassiniorbiterinstruments/nstrumentscassinirpws/images/rpws1.jpg

fixed-bias measurements, though the latter are not of interest for this report. Usually sweeps are performed with a bias voltage between −32 V and +32 V and the current is measured in 256 of 512 steps within about 0.5 s. Around the moon Titan a bias voltage range of ±4 V is often used to increase the resolution. In normal operation such sweeps are performed every 10 min, but in interesting regions, such as flybys of Saturn's moons, measurements can be performed every 24 s. A theoretical voltage-current characteristic curve is fitted to the weep data to determine the plasma parameters. Figure 4 shows a LP sweep from the Langmuir probe on-board the Cassini spacecraft together with the fitted curve.

For this study of Saturn's magnetosphere not the direct measurements of the LP were used to derive the electron density, instead the floating potential of the LP (U_{float}) was used [MMW+09]. This method is more appropriate in a tenuous plasma, like in Saturn's magnetosphere. Photoelectrons escaping from the spacecraft are balanced by the plasma electrons it collects. This means that the s/c ends up more and more positive the less plasma electrons there are, as it has to drag back a larger proportion of its own photoelectrons to balance the current. The LP is used to estimate the s/c potential, which is proportional to the floating potential. As the LP is mounted rather close to the spacecraft compared to the Debye length, which can reach several hundred meters in Saturn's magnetosphere, the floating potential of the LP can be used to determine the ambient electron number density N_e. Calibration of the U_{float} measurements to plasma density was done during Cassini Saturn orbit injection (SOI) using the electron spectrometer data of CAPS/ELS on-board Cassini.

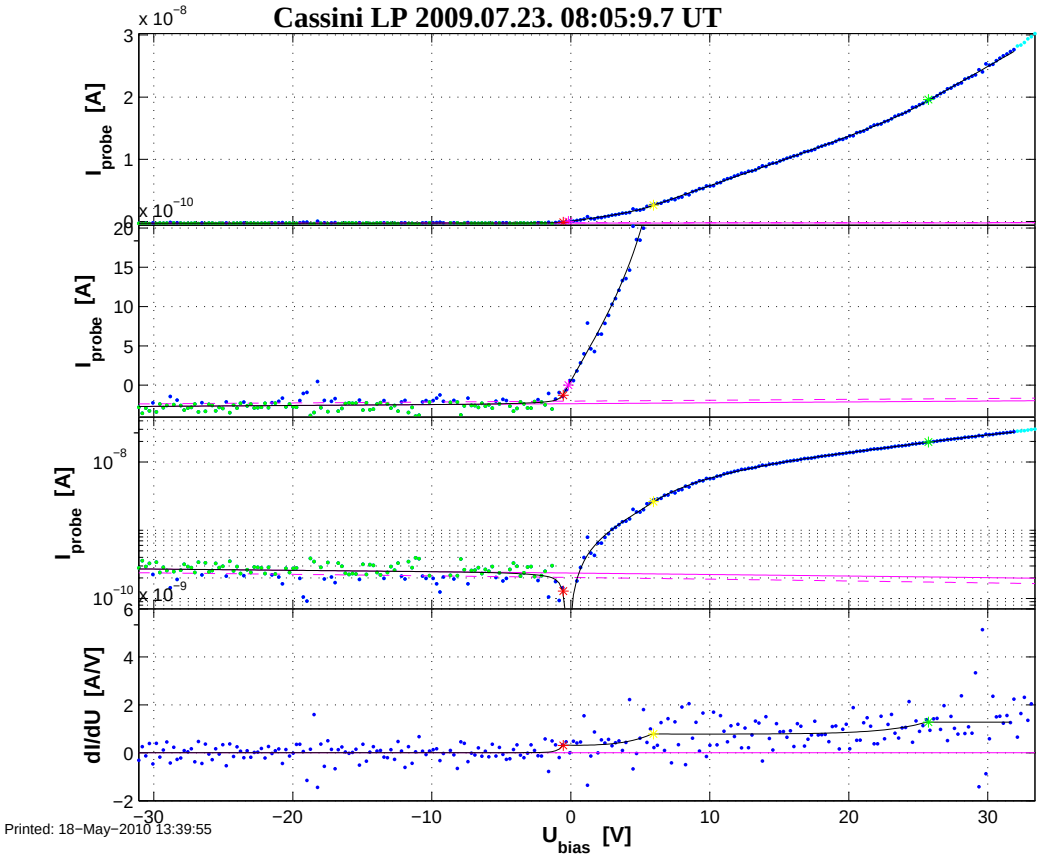

Figure 4: Typical Langmuir probe sweep, the left part ($U_{bias} < 0$) is dominated by ions, whereas on the right part ($U_{bias} > 0$) the current is mainly caused by electrons. The upper three panels show the current to the probe dependent on the bias voltage. The lower shows the derivative $\frac{dI}{dU}$. The floating potential U_{float} is marked with a red star $*$.

3 Analysis

As described in section 2.3 the LP floating potential was used to derive the ambient electron number density. The extraction of the floating potential from sweeps was done using a standard software package of the IRFU, it was an improved version of that one used in in the paper of Morooka et al. [MMW+09]. As relationship between U_{float} and N_e the same function as in the paper of Morooka et al. was used. The function consists of two exponentials and is given by

$$N_e = 0.03 \exp\left(-\frac{U_{float}}{2.25}\right) + 0.50 \exp\left(-\frac{U_{float}}{0.47}\right) \quad (1)$$

where U_{float} is in volts and N_e in cm^{-3}. This proxy relation has an accuracy of about a factor two in absolute density and can be used for data that give plasma densities below $5\,\mathrm{cm}^{-3}$.

For the analysis also magnetometer data from MAG on-board Cassini were used to find a correlation between variations in density and magnetic field. The MAG data were also used to find Saturn's magnetopause and eliminate data outside the magnetosphere, see also section 3.3 and figure 8.

For this report the data from orbit 099 to 126 were analysed, which covers the whole year 2009 and the beginning of 2010, i.e. the time around Saturn's equinox on 11 August 2009.

3.1 Dependence on EUV intensity

As described in section 2.3 the floating potential, from which the electron density was derived, depends not only on the ambient plasma density, it depends also on the solar radiation which releases electrons from the spacecraft by the photoelectric effect. The spacecraft gets more negative when the solar EUV irradiation is higher, since more s/c photoelectrons are released. A measure for the activity of the Sun in the EUV range is the F10.7 index. It gives the flux of solar radiation with a wavelength of 10.7 cm and is measured in $10^{-22}\,\mathrm{W\,m^{-2}\,Hz^{-1}}$.

During the SOI in 2004, the F10.7 index was about 1.2, in 2009 it was around 0.8, which is due to change of solar activity. For the calibration and finding of (1) data from the SOI were used. To see the effect of the solar EUV intensity on the floating potential, the floating potentials in the solar wind outside Saturn's magnetosphere were compared. The F10.7 index and the floating potential U_{float} for different measurement intervals are shown in figure 5.

There is no clear relation between the solar F10.7 index and the LP floating potential in the solar wind visible. There might be a trend hidden in the large variation of the floating potential, but it is difficult to find a correction for the density derived from the floating potential. So calibration (1) is used for this study.

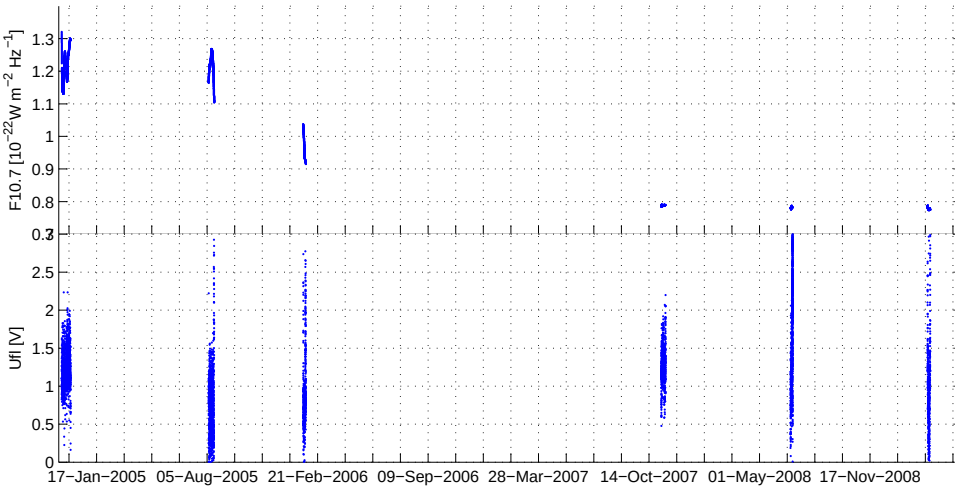

Figure 5: F10.7 index and LP floating potential for selected time intervals where Cassini was outside Saturn's magnetosphere

3.2 Dependence on spacecraft attitude

The attitude of the spacecraft has a large effect on the spacecraft potential. The s/c surface exposed to sunlight depends on the s/c attitude relative to the direction of the Sun. This gives a change in photoelectron emission, meaning that for a given density, the s/c need not go so positive when exposing its ends to the Sun as when the sides are facing the Sun.

Another s/c attitude dependent effect is due to the LP itself. If the LP is sunlit, the photoelectron current from it is high because many electrons are released from the probe, whereas the photoelectron current is very low if the probe is in shadow. Shadow on the Langmuir probe can be caused by objects between the spacecraft and the Sun, or by the spacecraft itself due to its attitude.

The exact effect of the spacecraft attitude on the spacecraft potential and the LP measurements is very complicated and has not yet been studied in detail. But one can find an empirical relation by analysing the LP measurements from different attitudes. This was done in previous studies, the results are included in the program of M. W. Morooka that derives the floating potential from a LP sweep.

To describe the s/c attitude, i.e. the s/c orientation in space, two different right-handed Cartesian coordinate systems are used. One of them is the coordinate system on the spacecraft itself, denoted as $X_{s/c}$, $Y_{s/c}$ and $Z_{s/c}$. The directions are shown in figure 3. In this coordinate system the Langmuir probe is mounted approximately in $-X_{s/c}$-direction.

The other coordinate system used is the Saturn Solar Ecliptic (SSE) reference system which has its origin in the centre of Saturn and is defined as:

X_{SSE} points from the centre of Saturn to the centre of the sun.
Y_{SSE} is given by the cross product of Z_{SSE} and X_{SSE}.
Z_{SSE} is parallel to the normal of the orbital plane of Saturn, directed northward.

For this study the unit vectors $X_{s/c}$, $Y_{s/c}$ and $Z_{s/c}$ are expressed in X_{SSE}, Y_{SSE} and Z_{SSE}, hence the spacecraft attitude is described by nine parameters. For measurements with the Langmuir probe, the orientation of the spacecraft relative to the direction of the Sun is crucial, i.e. the projection of $X_{s/c}$, $Y_{s/c}$ and $Z_{s/c}$ on X_{SSE} are the important quantities for the analysis.

The measurements have been corrected for the spacecraft attitude, but there seems to be still a large effect when the $Z_{s/c}$-axis points away from the Sun. In this configuration the Langmuir probe and the most part of the spacecraft is in the shadow of the large antenna of the spacecraft (white dish in figure 3). For projections smaller than -0.994 of $Z_{s/c}$ on X_{SSE}, i.e. angles larger than 173.7 ° between $Z_{s/c}$ and X_{SSE} the measurements differ significantly from measurements with other spacecraft attitudes, see figure 6. However this was not observed for all data points with a corresponding s/c attitude, but to be sure all measurements with projections smaller than -0.994 of $Z_{s/c}$ on X_{SSE} (plotted in red in figure 7) were removed from the analysis. The effect of the spacecraft attitude should be investigated in more detail in order to keep all valid data.

3.3 Selecting the data

The data from the LP were selected for analysis by the following criteria:

- Not closer than 7 Saturn radii to Saturn or 10 Titan radii to Titan.
- Obtained electron density is below $5\,\mathrm{cm}^{-3}$.
- Data were taken inside Saturn's magnetosphere, manually selected time intervals.
- Electron temperature T_e larger than 0.01 eV.
- Fit of sweep curve deviates not too much from data points ($QQ > 1.5$).
- The angle between the spacecraft $Z_{s/c}$-axis and the direction of the Sun is below 173.7 °.

The reasons for this selection are explained in the following.

The inner magnetosphere of Saturn and the ionosphere of the moon Titan are regions with dense plasma. In these regions the Debye length becomes small ($\lesssim 1\,\mathrm{m}$) and the proxy method does not work well. The ions then start to play a role for the spacecraft current balance, whereas in the outer magnetosphere, only plasma electrons and photoemission are important. In this study, relation (1) is used to derive the electron number density around the spacecraft. This formula is only valid for low densities (lower than about $5\,\mathrm{cm}^{-3}$ [MMW+09]). This is the reason, why regions closer

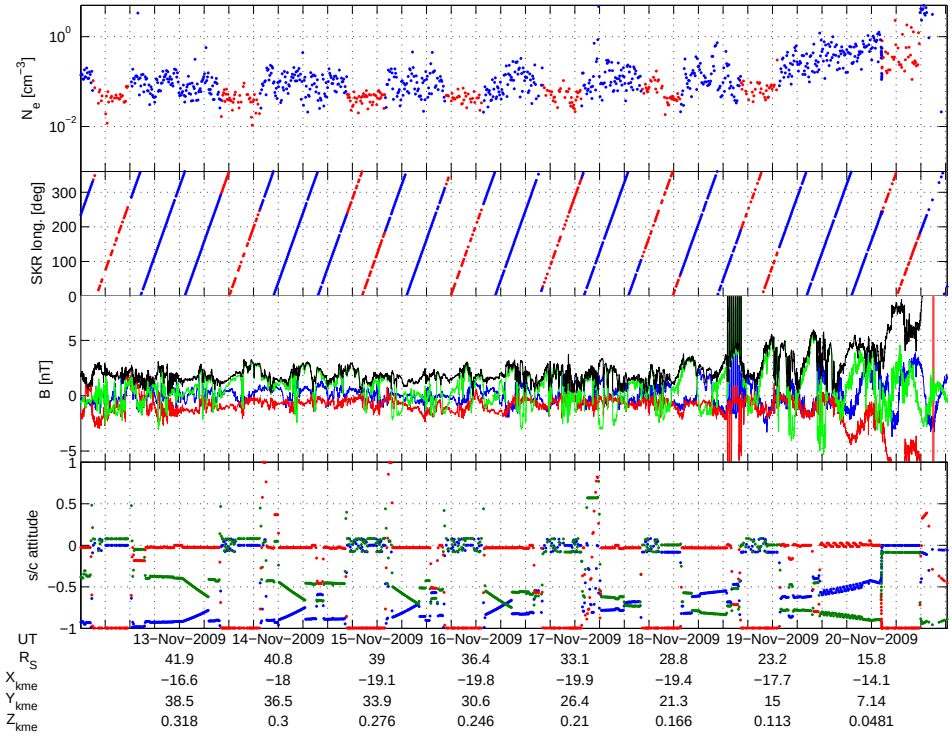

Figure 6: Data from orbit 121, the upper panel shows the electron density obtained from the floating potential. The second panel shows the SKR longitude of Cassini. The blue dots are valid data points, whereas the red dots may be incorrect. There seems to be a correlation between the obtained density and the s/c attitude, cf. lower panel. The third panel shows the magnetic field from MAG, blue for B_ϕ, red for B_z, green for B_r and black for $|B|$, measured in spherical KME coordinates. The lower panel shows the spacecraft attitude, the values are the cosine of the angle between the s/c axes and the direction of the Sun, blue for $X_{s/c}$, green for $Y_{s/c}$ and red for $Z_{s/c}$.

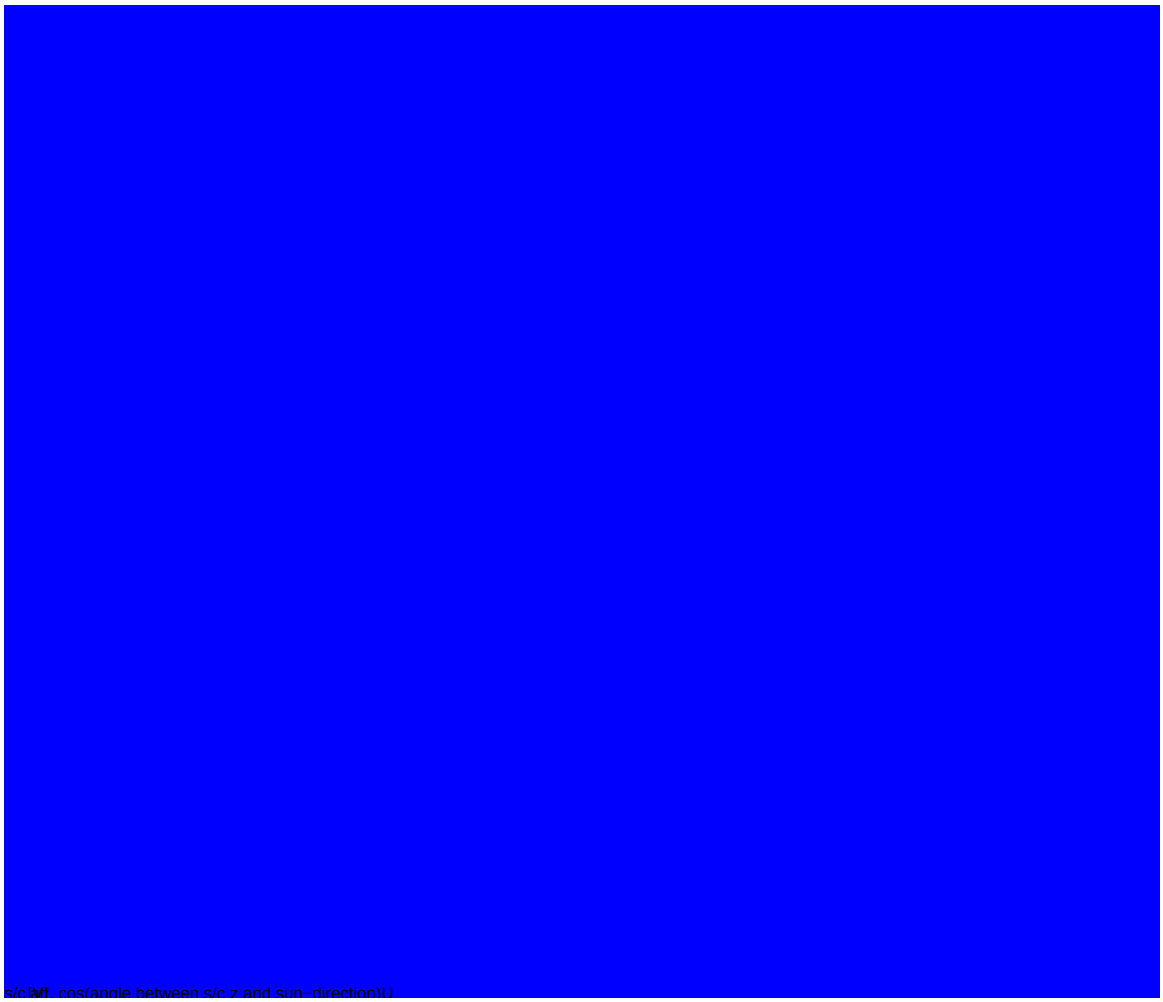

Figure 7: Measured floating potential dependent on the spacecraft attitude, the data are from orbit 099 to 126. The blue data points were used for the analysis, whereas the red data points were eliminated, for these is the angle between $Z_{s/c}$ and the direction to the sun larger than 173.7 °.

than 7 Saturn radii to Saturn and closer than 10 Titan radii from Titan were excluded from the analysis, as well as measurements that result in a density higher than $5\,\mathrm{cm}^{-3}$.

As we want to study the electron density in Saturn's magnetosphere, data points outside the magnetosphere were excluded from the analysis. The extension of the magnetosphere varies quite a lot, which is the reason for a manual elimination of data outside the magnetosphere (i.e. in magnetopause and solar wind). In addition the fluctuation of the magnetic field has a much higher frequency in the magnetosheath than inside the magnetosphere. The direction of the magnetic field can also be used to find the boundary of Saturn's magnetosphere. That is the reason why also MAG data were used to find data outside Saturn's magnetosphere. The elimination was done manually by choosing time intervals where Cassini was for sure inside the magnetosphere. Figure 8 shows the density measurements using the LP floating potential and the MAG data from parts of orbit 104 and 105. The magnetosheath is clearly visible as a relatively constant electron density of about $10^{-1}\,\mathrm{cm}^{-3}$ as well as high frequency variations of the magnetic field.

In addition densities from a fit that deviates too much from the real data of the current-characteristic were eliminated in the analysis, as well as data with an electron temperature below $10^{-2}\,\mathrm{eV}$. Data points with a s/c attitude such that the $Z_{s/c}$ is almost pointing away from the Sun were also eliminated, see section 3.2.

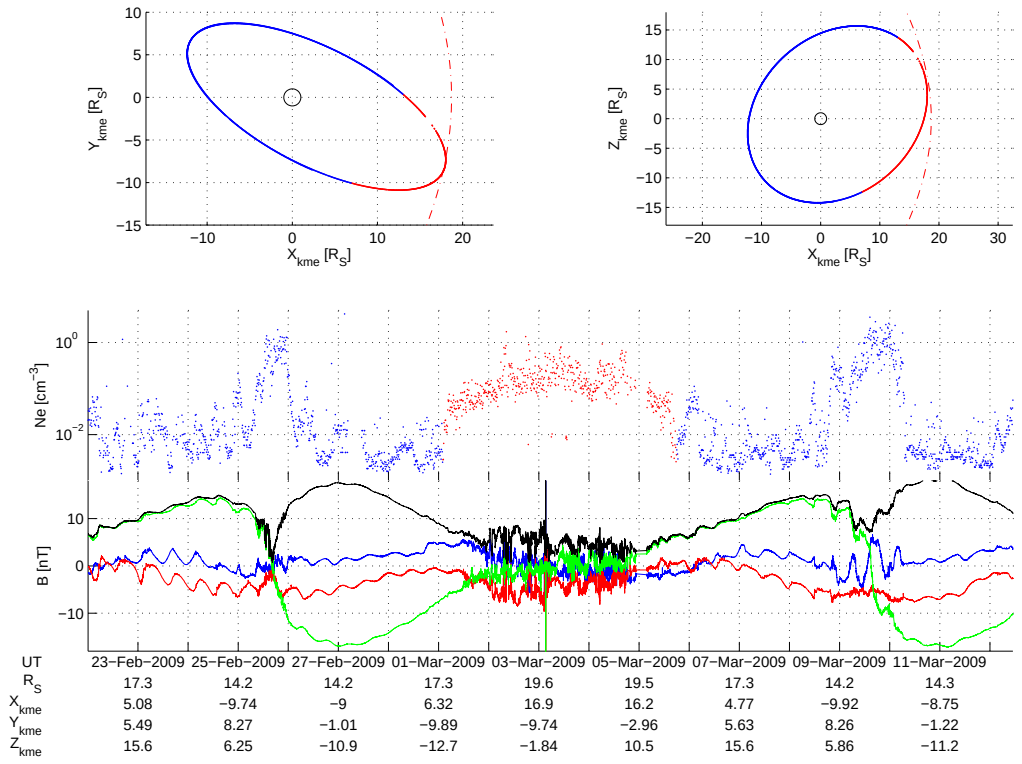

Figure 8: Data from orbit 104 and 105. The spacecraft trajectory is shown in the upper panels. The dash-dotted lines show the typical position of Saturn's magnetopause. The middle panel shows the electron density obtained from the floating potential. The data points in red are probably outside Saturn's magnetosphere and are eliminated in the analysis. The lower panel shows the magnetic field obtained by MAG, blue for the azimuthal component B_ϕ, red for B_z, green for B_r and black for the total magnetic field $|B|$, measured in the KME spherical coordinates.

4 Results

4.1 General characteristics

For this study data from December 31, 2008 to February 22, 2010 (orbits 099 to 126) were analysed. The local time (LT) and magnetic dipole L-value coverage of the density data from Cassini is shown in figure 9. The colours of the data points indicate the location of Cassini above/below the equatorial region. Most of the data used in the analysis are from the nightside and the dusk region. Unfortunately there are only few data on the dayside, especially around the equatorial region. This distribution should be kept in mind when interpreting the data, since the analysis of the radial distribution in the next section includes only data points from the equatorial region (red in figure 9), i.e. almost only data with $20 \lesssim \mathrm{LT} \lesssim 22$ for the nightside.

The orbital trajectories in $\sqrt{X_{kme}^2 + Y_{kme}^2}$ and Z_{kme} are shown in figure 10. Compared with the statistics from Morooka et al., we have more data points from high latitudes. The density along the spacecraft trajectory is colour-coded. The figure shows a high electron density around the equatorial plane which decreases with increasing distance from Saturn as well as with increasing distance from the equatorial plane. The plasma is mainly located in a region with $|Z_{kme}| \lesssim 5\,\mathrm{R_S}$ and $R \lesssim 20\,\mathrm{R_S}$. A possible position of the plasmapause is marked with grey.

The electron density shows a longitudinal variation with a periodicity of about 10 h, similar to that of the Saturn kilometric radiation (SKR), see section 4.4. Saturn is the source of long wavelength radio emissions, the Saturn kilometric radiation. The modulation of this radiation is assumed to be due to Saturn's rotation. The SKR can be used to define a longitude system [KLA+07]. The density variation due to SKR longitude is also consistent with previous studies [MMW+09].

4.2 R dependence

The electron density in Saturn's magnetosphere shows a dependence on the distance from Saturn which can be seen in figure 10 and 11. The density decreases with increasing distance from Saturn. Figure 11 shows the density profile in the equatorial region ($|Z| \leq 0.5\,\mathrm{R_S}$), the upper panel shows data from the dayside ($8 < \mathrm{LT} < 16$), middle and lower panel show data from the nightside ($20 < \mathrm{LT} < 4$). The data from orbit 121 are plotted in cyan, they show a lower density than the other orbits on the dayside at distances between $11\,\mathrm{R_S}$ and $13\,\mathrm{R_S}$. The reason for that is not clear, maybe it is the magnetospheric interaction region. In this region, cool and dense plasma is moving outward and hot and tenuous plasma is moving inward, so called interchange injections [HRB+05] [BGH+05]. This could be an explanation for the fluctuation and deviation from the other data.

Data from orbit 103 and 104 are plotted in green in the second panel. At a distance of about $12\,\mathrm{R_S}$ from Saturn, the densities for these orbits were significantly lower than the other data. This may also be the effect of interchange injections.

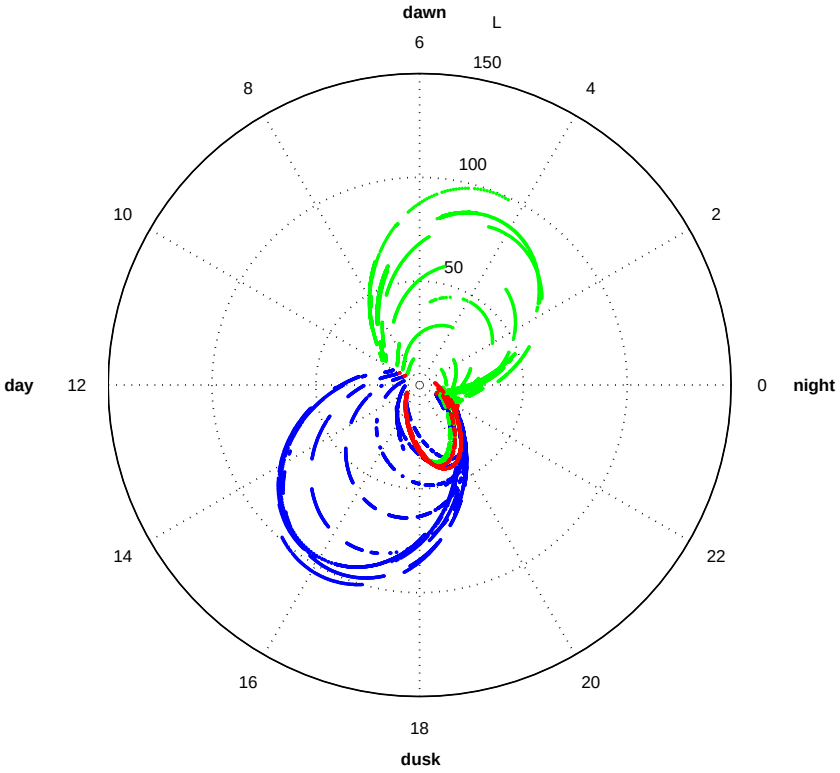

Figure 9: Local time coverage of the data used in this study, projected along the magnetic dipole field lines on the equatorial plane. The direction of the Sun is at at 12 h, the L-values are measured in Saturn radii. Data points from the northern hemisphere ($Z > 0.5\,\mathrm{R_S}$) are plotted in blue, data points from the southern hemisphere ($Z < 0.5\,\mathrm{R_S}$) are plotted in green and data from the equatorial region ($|Z| \leq 0.5\,\mathrm{R_S}$) are plotted in red.

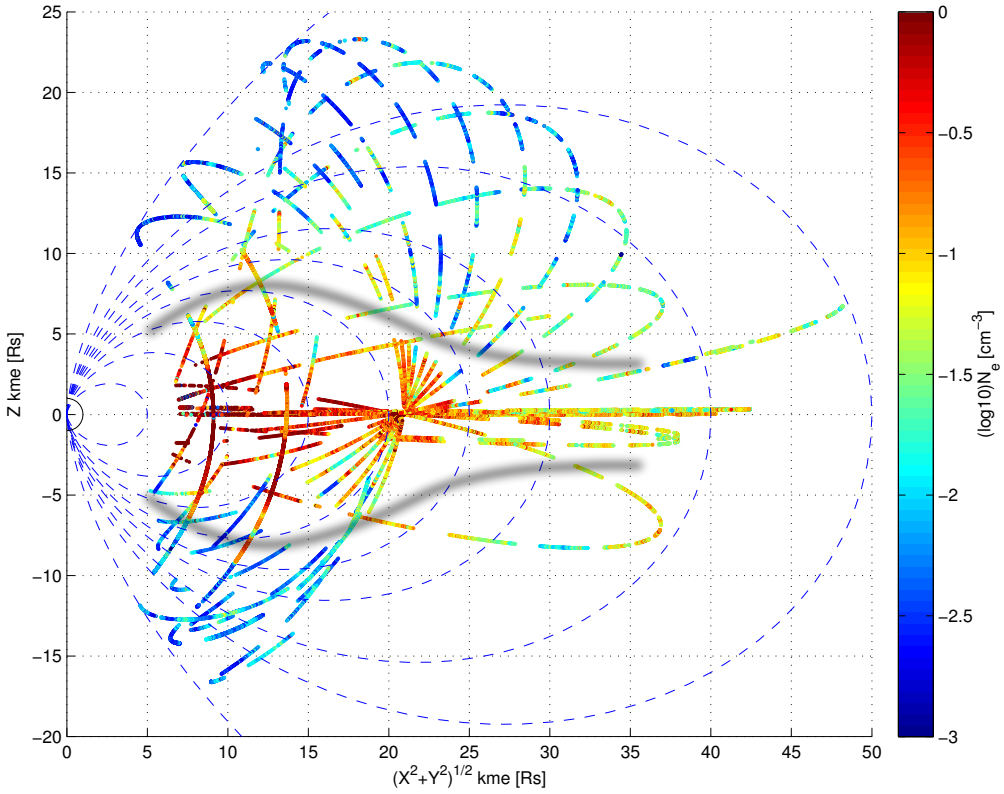

Figure 10: Electron density along the Cassini orbits (099-126) used in this study. The blue dashed lines show the magnetic dipole field lines for L=5, 10, 15, 20, 25, 30, 40, 50 and 100, the L-value gives the the radial distance in Saturn radii where a magnetic field line crosses the equator. A possible position of the plasmapause is plotted in grey.

Despite data from Titan passes (closer than $10\,R_T$ to Titan) were eliminated, the data points around $20\,R_S$ in all panels show an increased density. It seems that Titan has an effect on the plasma density even at distances larger than 10 Titan radii from Titan.

The data points closer than $11\,R_S$ from Saturn show a large fluctuation of the density, this could be due to interchange injections. Interchanging flux tubes can penetrate deep into the magnetosphere, bringing in a density cavity and hot plasma [BGH+05] [HRB+05]. The evolution of such interchange fingers is difficult to describe and could explain the scattering of the data.

The magenta dashed line shows the theoretical density due to the model of Persoon et al. [PGK+05],

$$N_e = 5.5 \cdot 10^4\, R^{-4.14} \tag{2}$$

where N_e is measured in cm^{-3} and R in Saturn radii R_S. The lines in blue and green represent the upper and lower limit for the measured density, the blue line varies as $7 \cdot 10^3\, R^{-3}$ and the green one as $1 \cdot 10^4\, R^{-4}$. The lower limit is much flatter than in the paper of Morooka et al. [MMW+09] where it was found as $6 \cdot 10^6\, R^{-7}$. The reason for that could be the different seasons of Saturn in the two studies, in this study the data were taken around Saturn's equinox. During equinox, Saturn's equatorial plane is aligned with the solar wind, i.e. there is no force of the solar wind that pushes the plasma in the equatorial plane to higher or lower latitudes. As result, the plasma sheet is located closer to the equator, even at large distances. The density in the equatorial plane decreases in this case because of the density decease within the plasma sheet with increasing distance from Saturn. In the case of the study of Morooka et al. the plasma sheet was curved an less aligned with the equatorial plane (see figure 2), thus the density in the equatorial plane decreased because of two effects, the density decrease within the plasma sheet with increasing distance from Saturn and the increasing distance from the centre of the sheet with increasing distance from Saturn. These two effects cause a faster decreasing of the density with increasing distance from Saturn, i.e. a smaller slope in a plot like figure 11.

In the middle and lower panel of figure 11 it seems that the density gets almost constant at distances beyond $30\,R_S$. This is consistent with the study of Morooka et al. and indicates a smaller effect of the centrifugal force at distances beyond $30\,R_S$.

4.3 Z dependence

4.3.1 Inner magnetosphere

The plasma in Saturn's inner magnetosphere is mainly located in the equatorial region. The measurements from orbit 099 to 126 and for a dipole L-value smaller than 16 can be seen in figure 12. The upper panel shows the the measurements on the dayside (local time between 8 and 16) and the lower panel shows the data from the nightside (local time smaller than 4 or larger than 20).

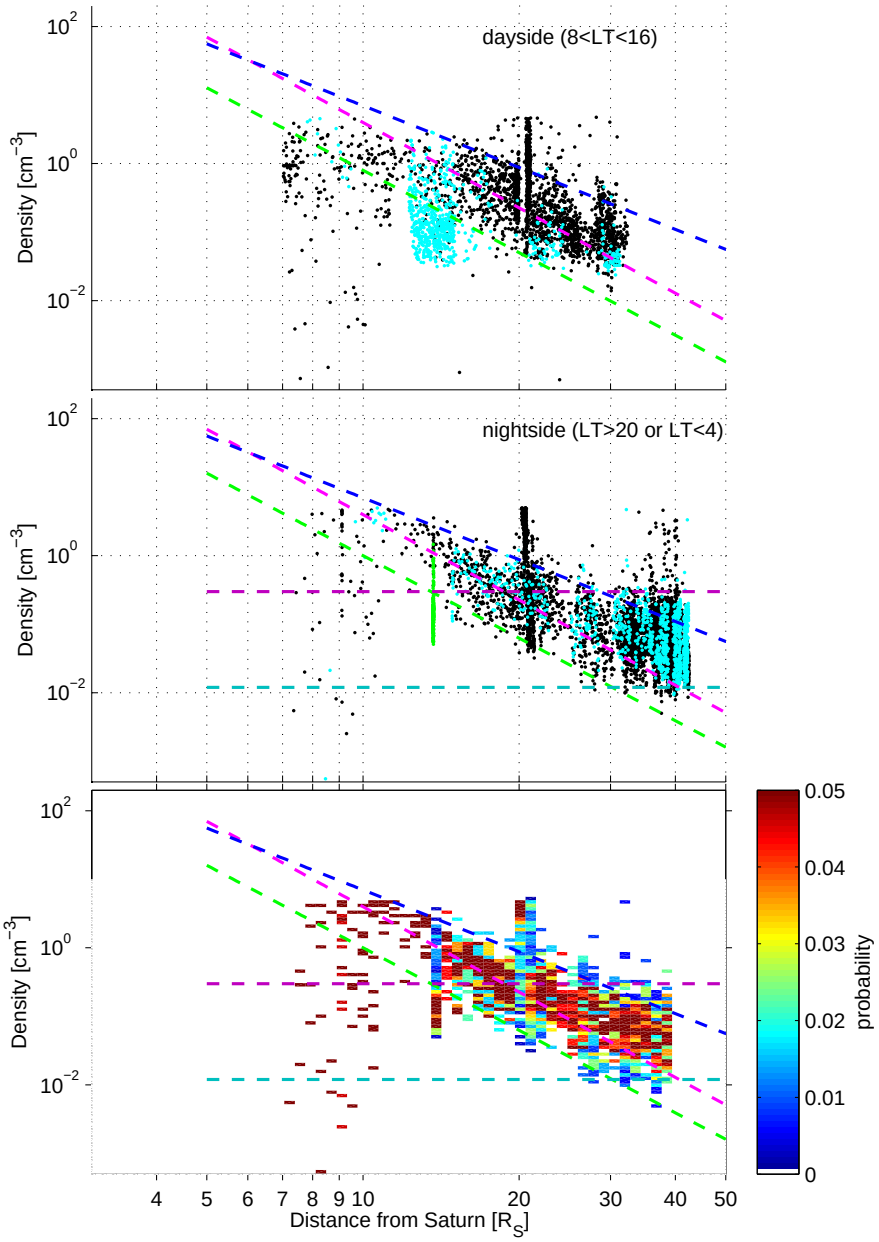

Figure 11: Density distribution with distance from Saturn in the equatorial plane ($|Z| \leq 0.5\,\mathrm{R_S}$). The data points in green are from orbit 103 and 104 (February 8, 2009 to March 3, 2009) and show a lower density at about $12\,\mathrm{R_S}$. The data points from orbit 121 are plotted in cyan, they differ from the the others on the dayside around $12\,\mathrm{R_S}$.

The data indicate that the plasma is mainly located in the equatorial plane, i.e. around $Z_{kme} = 0$. The density distribution can be approximated by an exponential function

$$N_e = N_0 \exp\left(-\left(\frac{Z}{H}\right)^2\right) \tag{3}$$

with a height scale H of about $3\,\mathrm{R_S}$, this is slightly larger than in the study of Morooka et al. 2009 where it was found between 2.3 and $2.8\,\mathrm{R_S}$.

The cyan data points in the range of $-1.4\,\mathrm{R_S} \lesssim Z_{kme} \lesssim 1.4\,\mathrm{R_S}$ are from orbit 103 (cf. green dots in figures 11) and show a lower density in the equatorial region. The reason is not clear, maybe it is due to the magnetospheric interaction region. It seems that orbit 103 was somehow special, the data differ much from the other measurements. Further investigations on orbit 103 should be done.

Since there are only few data points on the dayside it is very difficult to analyse the density distribution. It seems that the distribution is similar to that of the nightside (lower panel), the density decreases with increasing distance from the equatorial plane. This is consistent with the study of Morooka et al.. For a meaningful statistical analysis it is necessary to use more data.

4.3.2 Outer magnetosphere

The measurements from the nightside (20<LT<4) for dipole L-values between 15 and 25 and larger than 25 are shown in figure 13. The upper panels show the density depending on the distance from the equatorial plane. The green dots are from orbit 103, as mentioned above the measurements of this orbit seem to be somehow special. The lower panels show the probability distributions of the data points, the data from orbit 103 are eliminated.

The data in the left panels (15<L<25) show a relatively symmetric density distribution around the equatorial plane in the magnetospheric tail. The density decreases with increasing distance from the equatorial plane, at $Z = \pm 10\,\mathrm{R_S}$ the density is about two orders of magnitude lower than in the equatorial plane ($Z = 0$). A fit of an exponential function to the data varies as $\exp\left(-\left(\frac{Z}{5.45}\right)^2\right)$ in the northern hemisphere and and as $\exp\left(-\left(\frac{Z}{4.44}\right)^2\right)$ in the southern hemisphere, where Z is measured in Saturn radii. The larger height scale means that the plasma disc is thicker than in the inner magnetosphere where a height scale of about $3\,\mathrm{R_S}$ was found (cf. section 4.3.1). It seems that the centrifugal force from the co-rotation of the plasma has a a strong effect even beyond $15\,\mathrm{R_S}$, confining the plasma in the equatorial region.

In the more distant tail (right panels in figure 13) the density distribution shows no such nice dependence on the distance from the equatorial plane like for smaller dipole L-values. In the southern hemisphere there might be a sharp boundary at $Z \approx -7\,\mathrm{R_S}$ where the electron density decreases by more than one order of magnitude, this could

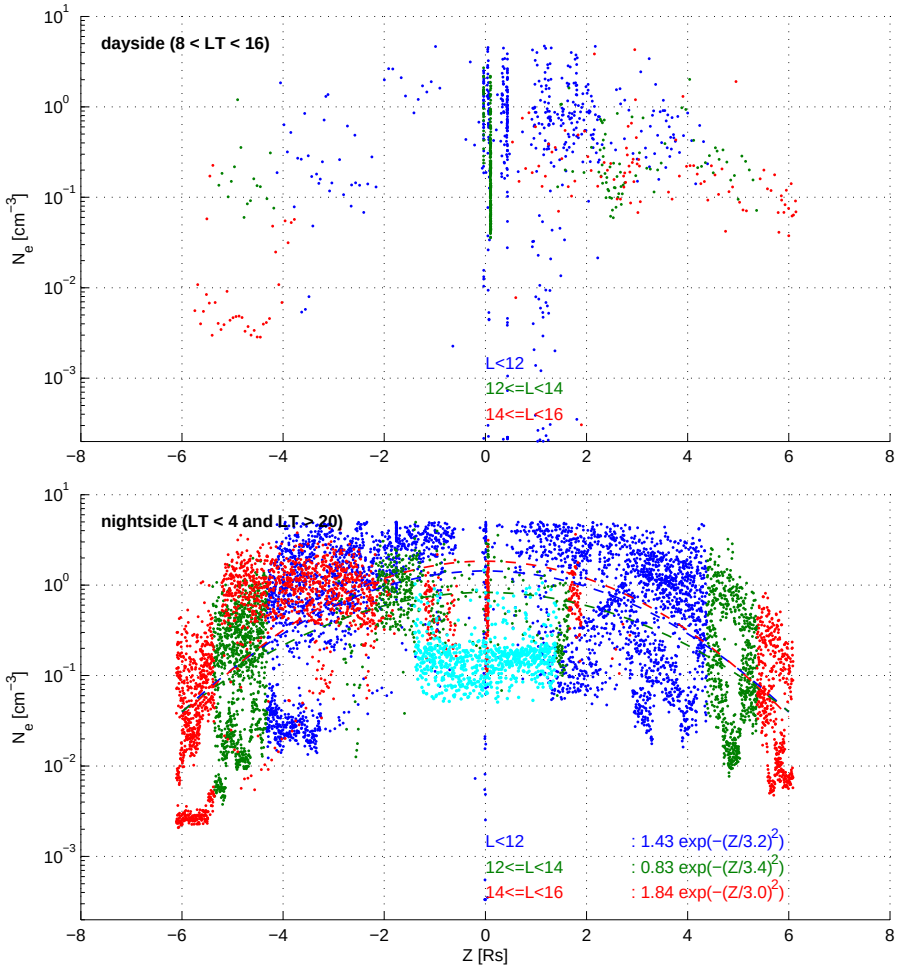

Figure 12: Density distribution with Z in the inner plasmasphere of Saturn for dipole L-values smaller than 16. Data points from orbit 103 with $|Z_{kme}| \leq 1.4\,\mathrm{R_S}$ are plotted in cyan.

be the outer boundary of the plasma sheet. Unfortunately there are no data points around $Z = -5\,\mathrm{R_S}$ to check the distribution in this region.

In the northern hemisphere the density decreases slower with increasing distance from the equatorial plane than for smaller L-values, the effect of the centrifugal force due to co-rotation seems to be less than in the inner magnetosphere. The boundary of the plasma sheet is probably between 6 and $13\,\mathrm{R_S}$, but it is difficult to see a clear trend because of the large fluctuation of the data.

4.4 Longitudinal asymmetry

Figure 2 in [MMW+09] shows a longitudinal asymmetry of the electron density in Saturn's magnetosphere. This is also visible in the data of some orbits used for this study. Figure 14 shows the data of the first part of orbit 115, the density (upper panel) varies by one to two orders of magnitude with a time period corresponding to Saturn's rotation ($\sim 10.7\,\mathrm{h}$). This is probably due to a longitudinal asymmetry co-rotating with Saturn, even at distances of more than $30\,\mathrm{R_S}$.

The red data points in the two upper panels may be invalid due to the spacecraft attitude, but for this special orbit it seems that the attitude correction works and one can trust the red data, too. The effect of the spacecraft attitude on the measurements with the LP (cf. section 3.2) has to be investigated further in order to eliminate only data points which are incorrect or better to correct these points for the spacecraft attitude.

The magnetic field measurements of MAG (third panel in figure 14) show also a variation corresponding to the density variation.

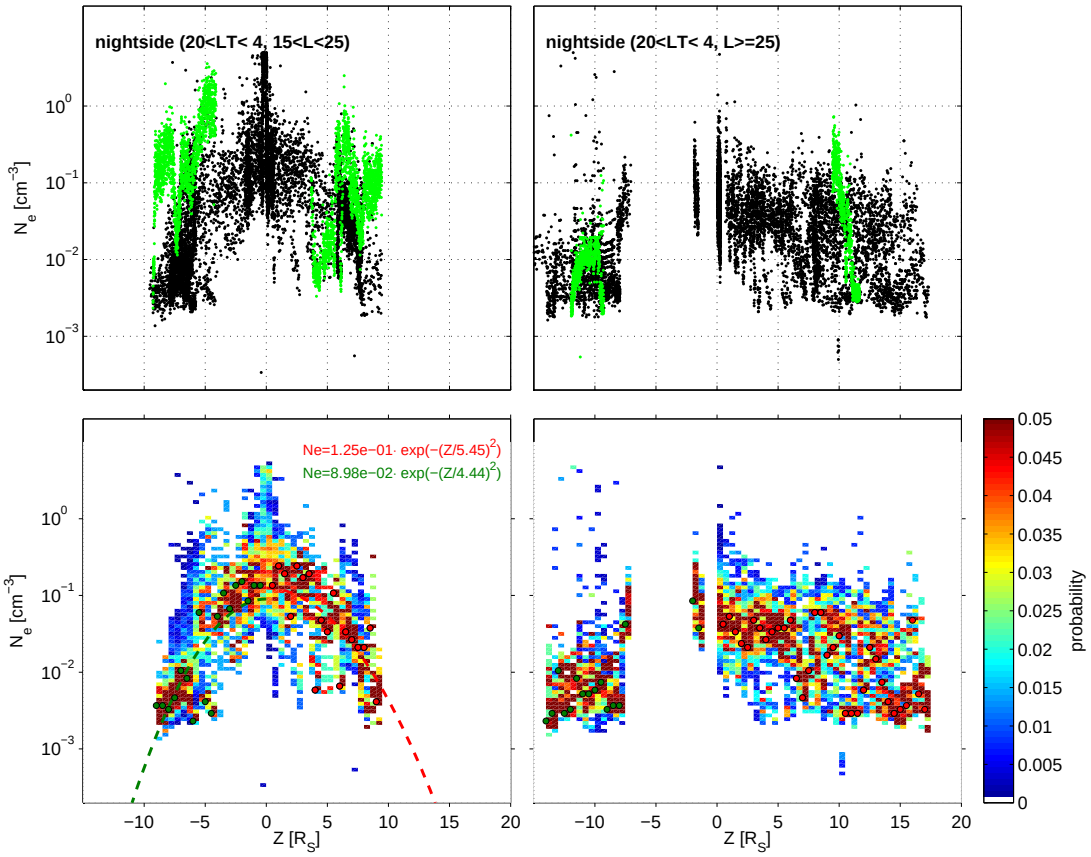

Figure 13: Density distribution with Z in the outer magnetosphere of Saturn for dipole L-values larger than 15. The green points in the upper panels are from orbit 103, they deviate from the measurements of the other orbits. They are eliminated in the lower panels. The points with the highest probability in the lower panels are marked with circles.

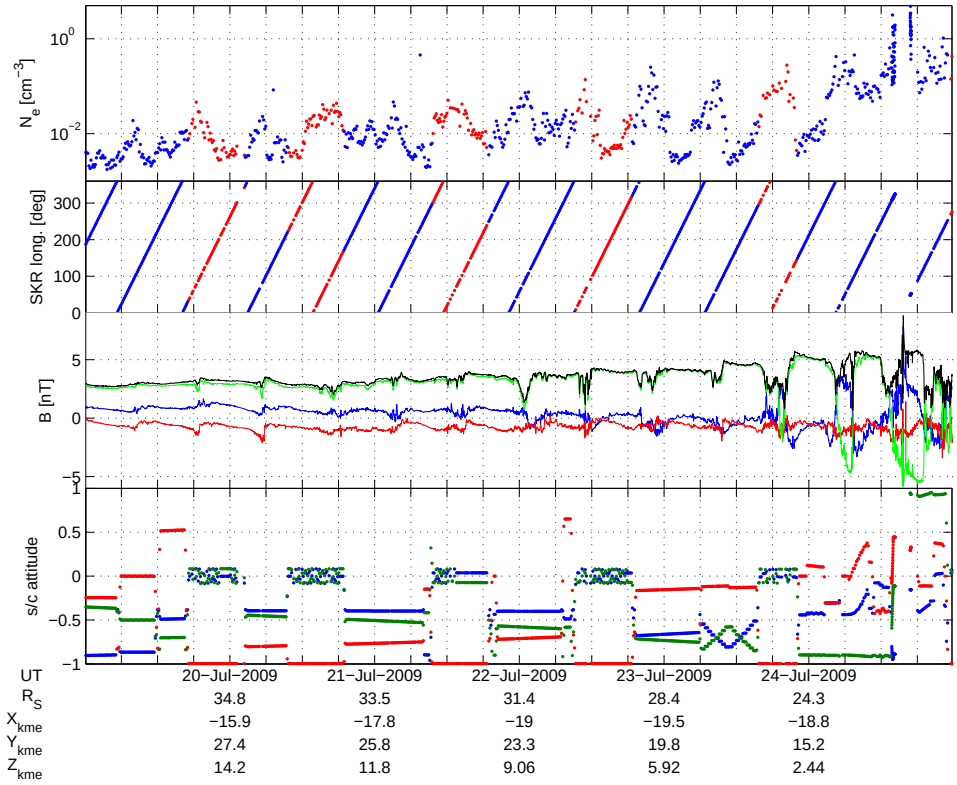

Figure 14: Data from orbit 115, the upper panel shows the electron density obtained using U_{float} and the second panel shows the SKR longitude of Cassini. The blue dots are valid data points, whereas the red dots may be invalid due to s/c attitude (cf. section 3.2). For this orbit it seems that the red data points are also valid, further investigations have to be done. The third panel shows the magnetic field measurements of MAG, blue for B_ϕ, red for B_z, green for B_r and black for $|B|$, measured in spherical KME coordinates. The lower panel shows the spacecraft attitude, the values are the cosine of the angle between the s/c axes and the direction of the Sun, blue for $X_{s/c}$, green for $Y_{s/c}$ and red for $Z_{s/c}$.

5 Summary and discussion

This study showed the main characteristics of the electron distribution in Saturn's magnetosphere and is consistent with previous studies. The plasma has a disc-like distribution with the highest density around the equatorial plane, decreasing with distance from the plane as well as with increasing distance from Saturn. This is due to centrifugal forces which occur because of the fast co-rotation of Saturn's magnetosphere. The disc-like structure was also found in the study of Persoon et al. [PGK+05] and Morooka et al. [MMW+09]. In the present study the plasma disc was more aligned with the equatorial plane than in the study of Morooka et al., this is probably due to the seasonal dependence of the magnetosphere, cf. section 2.1.

The study also showed the difficulties with measurements on spacecraft, especially their dependence on parameters like the s/c attitude or the EUV intensity. It was not as easy as it may seem to correct the data for such effects and interpret the measurements correctly.

There were also data which looked not as expected, for example data in the equatorial region of orbit 103. Also data from orbit 121 deviate from the other data in the equatorial region on the dayside around 12 R_S from Saturn. This could be an effect of interacting injections [HRB+05] [BGH+05], but should be investigated further.

5.1 Improvements and further investigations

There are some improvements that could be done in this study. One of these is a better s/c attitude correction. In this study many data points were eliminated when the spacecraft $Z_{s/c}$-axis was pointing almost away from the Sun (angle larger than 173.7 °), but not all measurements with such a configuration showed an unusual behaviour. This should be checked to avoid the elimination of valid data.

Another improvement would be a calibration of the dependence of the floating potential on the solar EUV intensity. For that one could use density data from CAPS/ELS and calibrate the density, but one has to be aware of the limited field of view and energy range of CAPS. The calibration should therefore be done in similar regions and with similar s/c attitudes.

In order to increase statistics, especially on the dayside, one should include more orbits in the analysis. But this would include data which are further away from equinox, thus giving another distribution. If the s/c attitude correction would be done better and data with all attitudes could be included in the analysis, the statistics would also be better.

There are some further investigations that could be done. In addition to the investigation of the orbits 103 and 121, the influence of the s/c attitude and the EUV dependence of the floating potential, one could make a model for the electron distribution around Saturn.

A List of abbreviations

ASI	Italian Space Agency
AU	Astronomic Unit
CAPS	Cassini Plasma Spectrometer
ESA	European Space Agency
EUV	Extreme Ultraviolet radiation
IRF	Swedish Institute of Space Physics
IRFU	Swedish Institute of Space Physics, Uppsala
KME	Kronocentric Magnetic Equator
LP	Langmuir probe
LT	Local Time
MAG	Magnetometer
NASA	National Aeronautics and Space Administration
N_e	Electron number density
RPWS	Radio and Plasma Wave Science
R_S	Radius of Saturn
R_T	Radius of Titan
s/c	Spacecraft
SKR	Saturn Kilometric Radiation
SOI	Saturn Orbit Injection
SSE	Saturn Solar Ecliptic
U_{bias}	Langmuir probe bias potential
U_{float}	Langmuir probe floating potential

References

[AKR+08] Arridge, C S. ; Khurana, K K. ; Russell, C T. ; Southwood, D J. ; Achilleos, N ; Dougherty, M K. ; Coates, A J. ; Leinweber, H K. ; Earth, At: Warping of Saturn's magnetospheric and magnetotail current sheets. In: *Journal of Geophysical Research* 113 (2008), Nr. A08217, S. 1–13. http://dx.doi.org/10.1029/2007JA012963. – DOI 10.1029/2007JA012963

[BGH+05] Burch, J L. ; Goldstein, J ; Hill, T W. ; Young, D T. ; Crary, F J. ; Coates, A J. ; Andre, N ; Kurth, W S.: Properties of local plasma injections in Saturn's magnetosphere. In: *Geophysical Research Letters* 32 (2005), Nr. L12S02, S. 3–6. http://dx.doi.org/10.1029/2005GL022611. – DOI 10.1029/2005GL022611

[GI10] Gombosi, Tamas I. ; Ingersoll, Andrew P.: Saturn: Atmosphere, Ionosphere, and Magnetosphere. In: *Science* 327 (2010), Nr. 5972, 1476-1479. http://dx.doi.org/10.1126/science.1179119. – DOI 10.1126/science.1179119

[Hol10] Holmberg, Madeleine: *Determination of Solar EUV Intensity and Ion Flux from Langmuir Probe Current Characteristics*. 2010 (UPTEC F)

[HRB+05] Hill, T W. ; Rymer, A M. ; Burch, J L. ; Crary, F J. ; Young, D T. ; Thomsen, M F. ; Delapp, D ; Andre, N ; Coates, A J. ; Lewis, G R.: Evidence for rotationally driven plasma transport in Saturn's magnetosphere. 32 (2005), S. 2–5. http://dx.doi.org/10.1029/2005GL022620. – DOI 10.1029/2005GL022620

[JPL] JPL: *Cassini Orbiter Instruments*. – http://saturn.jpl.nasa.gov/spacecraft/cassiniorbiterinstruments/

[KLA+07] Kurth, W S. ; Lecacheux, A ; Averkamp, T F. ; Groene, J B. ; Gurnett, D A. ; Lecacheux, A: A Saturnian longitude system based on a variable kilometric radiation period. In: *Geophysical Research Letters* 34 (2007), Nr. L02201, S. 10–13. http://dx.doi.org/10.1029/2006GL028336. – DOI 10.1029/2006GL028336

[MMW+09] Morooka, M. W. ; Modolo, R. ; Wahlund, J.-E. ; André, M. ; Eriksson, A. I. ; Persoon, A. M. ; Gurnett, D. A. ; Kurth, W. S. ; Coates, A. J. ; Lewis, G. R. ; Khurana, K. K. ; Dougherty, M.: The electron density of Saturn's magnetosphere. In: *Annales Geophysicae* 27 (2009), Nr. 7, 2971–2991. http://dx.doi.org/10.5194/angeo-27-2971-2009. – DOI 10.5194/angeo–27–2971–2009

[PGK+05] Persoon, A M. ; Gurnett, D A. ; Kurth, W S. ; Hospodarsky, G B. ; Groene, J B. ; Canu, P ; Dougherty, M K.: Equatorial electron density measurements in Saturn's inner magnetosphere, Geophys. In: *Geophysical Research Letters* 32 (2005), Nr. L23105. http://dx.doi.org/10.1029/2005GL024294. – DOI 10.1029/2005GL024294

[Sat09] *Saturn from Cassini-Huygens*. Springer Netherlands, 2009 . – ISBN 978–1–4020–9216–9 (Print) 978–1–4020–9217–6 (Online)